Iranian Journal of Microbiology
Volume 16 Number 3 (June 2024) 366-375

ORIGINAL ARTICLE

Antibacterial and antibiofilm activities of zingerone and niosomal zingerone against methicillin-resistant *Staphylococcus aureus* (MRSA)

Laleh Larijanian[1], Morvarid Shafiei[2*], Abdollah Ghasemi Pirbalouti[1], Atousa Ferdousi[1*], Mohsen Chiani[3]

[1]Department of Microbiology, Shahr-e-Qods Branch, Islamic Azad University, Tehran, Iran
[2]Department of Bacteriology, Pasteur Institute of Iran, Tehran, Iran
[3]Department of Nanobiotechnology, Pasteur Institute of Iran, Tehran, Iran

Received: December 2023**, Accepted:** May 2024

ABSTRACT

Background and Objectives: Methicillin-resistant *Staphylococcus aureus* (MRSA) is a major cause of nosocomial and community acquired infections. Nanoparticles are considered as proper tools to overcome the therapeutic problem of antimicrobial-resistant infections because of the drug concentration increment at the desired location and protection from enzymatic degradation. The goal of this study was to evaluate the effect of the antibacterial and antibiofilm activities of zingerone and niosome containing zingerone against pre-formed biofilm of MRSA isolates.

Materials and Methods: 62 MRSA isolates cultured from patients with diabetic ulcers were investigated. Niosomes were synthesized and characterized by X- ray diffraction, zeta potential and scanning electron microscopy (SEM). The size of niosomal particles measured by SEM and zetasizer.

Results: The surface charge of prepared niosomes was about -37 mV. The effect of the zingerone and noisome containing zingerone was evaluated against biofilms of MRSA isolates. Also, the antibiofilm activity of prepared niosomes on gene expression of MRSA biofilms was evaluated using Real Time PCR. Our results demonstrated that the niosome containing zingerone had a diameter of 196.1 nm and a -37.3-mV zeta potential. Zingerone removed one and three-day old biofilms of MRSA at the concentration of 1000 µg/ml, while the zingerone-laoded niosomes removed 1, 3- and 5-days old biofilms at the concentration of 250 µg/ml, 250 µg/ml, and 500 µg/ml.

Conclusion: The results indicated that niosome containing zingerone eliminated MRSA and its biofilms faster compared with free zingerone and it suggested that zingerone-encapsulated niosomes could be considered as a promising treatment against MRSA and its biofilms.

Keywords: Niosomes; Zingerone; Biofilm; Methicillin resistant *Staphylococcus aureus*

INTRODUCTION

Staphylococcus aureus is one of the most common causes of nosocomial infections, bedsores and diabetic wounds. *S. aureus* has become resistant to a extensive range of antibiotics including methicillin, which can be referred to as methicillin-resistant *Staphylococcus aureus* (1). Methicillin-resistant

*Corresponding authors: Morvarid Shafiei, Ph.D, Department of Bacteriology, Pasteur Institute of Iran, Tehran, Iran. Tel: +98-21-64112231 Fax: +98-21-66405535 Email: dr.m.shafiei@pasteur.ac.ir

Atousa Ferdousi, Ph.D, Department of Microbiology, Shahr-e-Qods Branch, Islamic Azad University, Tehran, Iran. Telefax: +98-21-4689000 Email: atousaferdousi@qodsiau.ac.ir

Staphylococcus aureus (MRSA) has a chromosomal fragment called staphylococcal cassette chromosome mec (SCCmec). SCCmec has the *mecA* gene encoding a binding protein with low affinity for penicillin (PBP2a) (2). Biofilm is one of the virulence factors in isolated MRSA, which provide protection against host immune responses and adverse environmental conditions (3). In fact, the ability to form biofilms is a suitable solution for the survival of microorganisms in excessive antimicrobial dosage, resulting to the emergence of resistant infections. This is due to the high resistance of cells within the biofilm to various antimicrobial compounds (4). The capacity of biofilm formation and antibiotic resistance of methicillin-resistant *S. aureus*, have made it a pathogen in the field of health (5). Biofilm production in *S. aureus* bacteria is due to activity of *ica* ABCD gene. Biofilm production leads to refractory infections, resulting in increased treatment costs and even failures in treatment and recurrence of infections (6). Minimum inhibitory and bactericidal concentrations (MIC and MBC) are standard criteria for antibiotic sensitivity tests and are used as an important reference in the treatment of acute infections (7). Common sensitivity assessment tests are not suitable for evaluation against bacterial biofilms, because free cells are used to determine the amount of MIC, while biofilm cells are more resistant to antibiotics than free cells (8). Niosome nanoparticles are carriers for drug delivery (9). They are a new way of delivering medication into bacterial cells and biofilms and have advantages over liposomes in terms of stability, storage time and better reproducibility than non-ionic surfactants (10). zingerone is a bioactive compound of ginger root. It is used in the food industry as a flavoring agent (11). Zingerone has different health medicinal benefits, including antibacterial and anti-biofilm (12). In this study, to enhance the antibacterial and antibiofilm activities of zingeron, zingeron loaded niosomes were synthetized. The anti-biofilm and antibacterial activitis of niosome containing zingerone and free zingerone were assayed against MRSA clinical strains isolated from diabetic wounds.

MATERIALS AND METHODS

Bacterial isolation and identification. Specimens were taken from diabetic wound exudates of patients hospitalized at Loghman Hospital in Tehran, Iran using sterile swab technique and transferred to Pasteur Institute of Iran. First, the isolates were diagnosed as *S. aureus* using biochemical tests (13). Also, the susceptibility of isolates to cefoxitin (30 µg) and oxacilin (1 µg) disks was assessed using disk diffusion method according to the Clinical and Laboratory Standard Institute (CLSI) guidelines (14). Notably, *S. aureus* ATCC6538 was used as MRSA controls.

***mecA* gene detection.** Bacterial DNA was extracted from cefoxitin-resistant *S. aureus* isolates using a DNA extraction kit (Qiagen, Hilden, Germany) according to the manufacturer's instructions. The final reaction volume was 25 µl containing 10 µl sterile distilled water, 12 µl of Taq DNA Polymerase Master Mix RED (AMPLIQON, Denmark), 1 µl of forward and reverse *mecA* primers (BIO NEER, Korea), and 1 µl of bacterial DNA Amplification of *mecA* gene, was carried out using GenePro thermal cycler (Bioer Technology, China) with the following cycling program: initial denaturation at 94ºC for 4 min, followed by 30 cycles at 94ºC for 45 sec, 58.5 ºC for 45 sec, and 72ºC for 1 min, with a final extension step of 72ºC for 3 min (Table 1). PCR products were electrophoresed on 1 % agarose gel, stained with DNA Green Viewer, and visualized using UV transillumination (Alpha Innotech, USA) (13, 14).

Biofilm formation assay. Microtitter plate test was used for biofilm formation assay. In Brief, an overnight culture of each isolate was grown in trypticase soy broth plus 0.2% glucose (Merck, Germany) for 24 h at 37ºC. The turbidity of growth in this medium was adjusted at 0.5 McFarland opacity using a spectrophotometer (Schimadzu, model UV-120-01, Japan) with the absorbance of 0.08-0.1 at 625 nm. Then, the bacterial suspensions (200 µl) were poured into a 96-well polystyrene microtiter plate (Sigma Aldrich, St. Louis, Missouri, USA) and incubated at 37ºC for 24 h without shaking followed by discardingof the supernantants of each well by aspiration. The wells were washed with sterile physiological saline (PBS, pH7.4) to eliminate all unappealing cells. Bacterials cells that adhered to the wells were fixed with absolute methanol for 10 min. The plates were stained with crystal violet (1%W/V). The excess stain was washed in tripilidcate the bound dye was resolubilized with 200 µl of glacial acetic acid (33%, v/v). The optical density of each well was calculated at 570 nm by ELISA reader. Uninoculated wells containing media were used as

Table 1. Minimmum Biofilm Eradication Concentration (MBEC) values of zingerone and niosome containing zingerone against one, three and five-day-old biofilms of MRSA isolates.

	MIC (µg /ml)	Minimmum Biofilm Eradication Concentration (MBEC) (µg /ml)		
		One-day old	Three-day old	Five-day old
Zingerone	512 ± 1	1000 ± 1	1000 ± 1	-
Zingerone-loaded niosomes	125 ± 1	250 ± 1	250 ± 1	500 ± 1

blanks (15). The optical density of ODs < 0.500, 0.500 < ODs < 1.500, ODs >1.500 was intended negative, positive, and strongly positive, respectively (15). All tests were performed in triplicates.

Preparation of niosomal zingerone. Thin layer hydration method was used to prepare niosome containing zingerone. First, span 60 (sorbitan monostearate), cholesterol, polyethylene glycol (PEG-3000) (Sigma, USA), and zingerone (Sigma, USA) with a molar ratio of 7:3:1:1 was mixed with 2:1 of a chloroform–methanol solution (16, 17). The control sample was prepared with the same formulation, except zingerone. The final mixture was stirred at 37ºC to achieve a homogenized suspension. The niosome suspension was transferred into a round-bottom flask and quietly spined at 100 rpm on a rotary evaporator (WB Eco Laborota 4000 Model, Heidolph Instruments, GmbH) at 60ºC to evaporation the organic solvent until a thin lipid film was settled on the wall of the flask. The final solid film was then dried fully by nitrogen gas and resuspended in 20 ml of 1 M phosphate buffer saline (PBS) with a pH value of 7.4, at 60ºC. All prepared batches were visually reviewed for opacity and flocculation in clear containers at 4ºC (18, 19).

Characterization of noisome: scanning electron microscopy (SEM). SEM (Quanta FEG 450, FEI USA) was employed to evaluate the uniformity, morphology, and size of niosomal zingerone based on the standards at the specialized laboratory of the Tehran University of Technology, Tehran, Iran. The samples were taped to SEM sample stub and coated with a 200 nm gold layer at 0.001 mmHg pressure (millimeters of mercury). Photographs were taken at a convenient magnification (20).

Determination of the particle size, size distribution and zeta potential of niosomal zingerone. Particle size, size distribution and zeta potential of niosome containing zingerone was analyzed using Zeta-sizer instrument (Nano ZS3600, Malvern Instruments Ltd., Worcestershire, UK) mobilized by a 633 nm He-Ne laser. The samples were analyzed at the same temperature, concentration and pH (25ºC, 0.1 mg ml^{-1}, pH7.4). The stability of niosomes was monitored for one month at 4ºC by measuring the polydispersity index, entrapment efficacy, zeta potential and particle size. The stability of niosomes was monitored during the storage condition (for 1 month at 4ºC) by measuring the particle size, polydispersity index, entrapment efficacy, zeta potential.

Zingerone entrapment efficiency. To investigate zingerone entrapment efficacy, followed up according to following (17, 19). Finally, the EE % of zingerone into the niosomal zingerone was determined by the following equation:

$$EE\ \% = \frac{\text{amount of initial drug} - \text{amount of unentrapped drug}}{\text{amount of initial drug}} \times 100$$

Zingerone release. Dialysis method was used to evaluate the release of zingerone from niosome containing zingerone followed up according to following (21).

Fourier transforms infrared spectroscopy (FTIR). Infrared transmission spectra of niosomes were analyzed using a spectrometer (Perkin–Elmer FTIR model 2000) in KBr disks from 4000 to 400 cm^{-1} (22). FTIR analysis identified absorption bands related to functional groups' vibrations in free zingerone, niosome containing zingerone and free niosome (as control). FTIR was used to investigate drug-ingredients interaction, compatibility, and structural features of samples (23).

Minimal inhibitory and bactericidal concentrations (MIC and MBC). The MIC and MBC of zing-

erone and zingerone-loaded niosomes against MRSA isolates were determined using the microtiter plate method according to CLSI standards (24).

Biofilm dispersion assay. A microtiter plate assay was used to determine the biofilm dispersion (21, 25). 20 µl of serially diluted bacterial suspension (1.5×10^8 CFU/mL) was applied to each well of sterile 96-well microtiter plates containing 180 µl of TSB medium. The plates were incubated for one day, three days and five days at 37ºC. Then, 200 µl of PBS (pH7.4) was used to wash off the non-adherent cells (26). Various dilutions of zingerone suspension and noisomal zingerone suspension were added to the wells. Blank niosome and medium alone (TSB + 0.1% of glucose) were used as negative control group. Three replicates were considered for each concentration. The plates were washed three times with PBS, and crystal violet (CV) was used to dye the biofilms. The absorbance was measured at 570 nm using an automatic ELISA reader (Titertek, R Multiscan, Germany) (27, 28).

Gene expression examination by real-time PCR. In order to analyse the effect of the zingerone and niosomes containing zingerone on MRSA biofilms, the expression levels of the *ica A* and *ica D* genes in MRSA (ATCC 6538) were assessed by real-time PCR (3, 29).

RNA extraction and cDNA synthesis. Extraction of RNA from biofilms was performed with RNX-Plus kit according to the manufature instruction (SinaColon Co. Iran). Then, synthesis of cDNA was carried out with cDNA synthesis Kit (Zist Fanavaran Co. Iran) (3, 29).

Real-time PCR performance. Quantitative real-time PCR was applied in a Light Cycler 96 Instrument with Roche Applied Science (Penzberg, Germany) with a SYBR Green kit (ABI. USA). All reaction tubes contained 2 µl of the cDNA, 0.5 µl of each of the forward and reverse primers, 10 µl SYBR green PCR master mix and 7 µl DEPC water. The reaction was started with an initial denaturation at 95°C for 5 min and 40 amplification cycles of 94°C for 20s, 60°C to 62°C (annealing temperature of *icaA, icaD* and 16S rRNA were 62°C, 60°C and 60°C, respectively) for 20 sec and 72°C for 20 sec. The formula $RQ= 2^{-\Delta\Delta Ct}$ was used to get relative gene expression in the comparative CT method and 16S rRNA was used as an internal control (3, 29).

Statistical analysis. One-way and two-way analysis of variance were used for statistical analysis (ANOVA) (Tukey test) (IBM SPSS Statistics 26.0.0.1 FP001 IF007) and Log-rank test for survival analysis by GraphPad Prism v. 9.0 software with a statistically significant p-value < 0.05.

Ethical approval. This study was approved by the Pasteur Institute of Iran ethics committee (IR.PII.REC.1400.086).

RESULTS

Isolation of MRSA. 98 of 160 clinical isolates were identified as *S. aureus*, according to the phenotypic and biochemical tests and 62 isolates were diagnosed as MRSA according to the results of anti-biogram tests and *mecA* gene PCR amplification.

Investigation of niosome properties. Based on the micrograph obtained from SEM, the niosome nanoparticles were spherical and almost identical in size. The size of niosomal particles measured by scanning electron microscopy was about 160 nm and the diameter measured by the zetasizer was about 196 nm (Fig. 1). Size distribution of niosome nanoparticles showed homogene dispersion for particles. Surface charge of niosome containing zingerone was about -37 mV. No significant difference was found in size, zeta potential, PDI and morphology between niosome containing zingerone and its control (zingerone free niosome).

Zingerone entrapment efficiency. The EE % of synthesized niosomes was obtained from an indirect method and using the zingerone standard curve equation. The results of our study demonstrated that EE% of niosome containing zingerone was about 69 %.

***In vitro* release study.** Our results showed that around 75% of zingerone (non-niosomal form or standard form) is released from dialysis bag after 15 hours, but only 30% of zingerone is released from the niosomal carrier after 36 hours. Comparative release of free zingeron and niosomal zingerone showed that zingerone in niosomal form is released at a slower rate than free zingerone (Fig. 2).

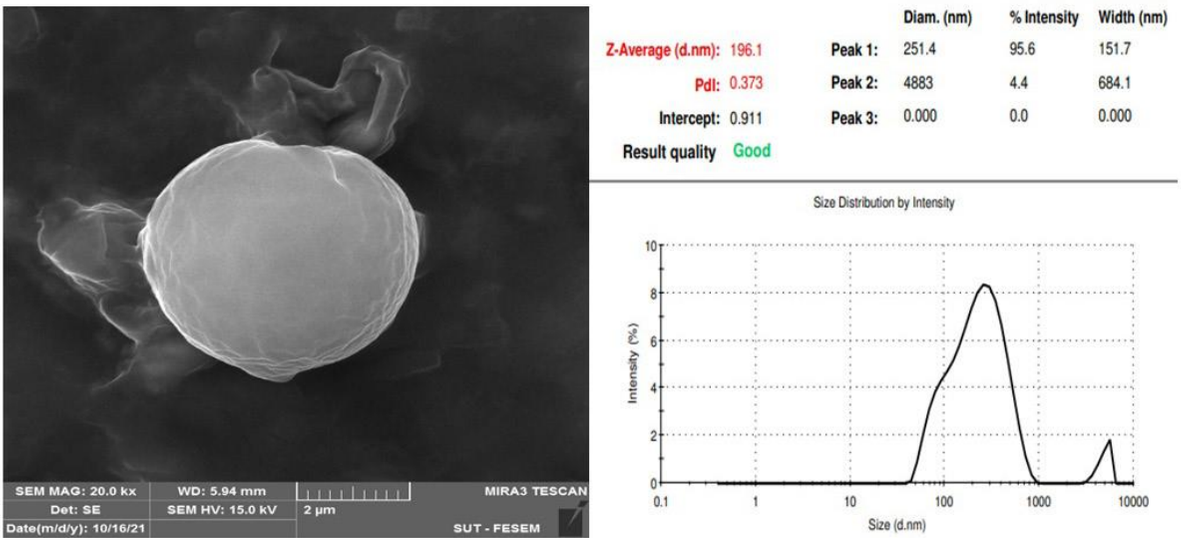

Fig. 1. SEM micrograph (left) and size distribution curve (right) of zingerone-loaded niosomes obtained by the dynamic light scattering method.

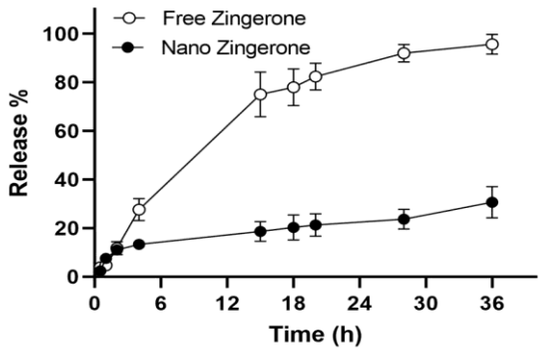

Fig. 2. Comparison of the release of zingerone from niosome and free zingerone at 37°C.

Fourier transform infrared spectroscopy. The spectra recorded for niosome with and without zingerone showed similar typical bands, indicating the characteristics in the backbone structure of the different substrates. It can be seen multiple complex absorption bands for zingerone in 457.27-1469.00 cm^{-1} because the molecular structure contains benzene ring. These bands are characteristics peaks related to zingerone. In addition, the wide peak in 3444.64 cm^{-1} was due to the hydroxyl group in the structure of zingerone. In the B pattern in (Fig. 3), a wide with medium intensity peak was observed in the 3435.54 cm^{-1} which is the characteristic hydroxyl groups in the niosome structure and similar band was observed in the C pattern 3422.64 cm^{-1} for niosome containing zingerone with preserving its structure. Also, sharp bands were observed in the 1737.17 cm^{-1} and 1576.28 cm^{-1} for stretching vibration of C=O functional groups in the niosome with and without zingerone, respectively. Relative wide peaks at 3435.54 cm^{-1} and 3422.64 cm^{-1} due to the hydroxyl group related to cholesterol in the niosome structure was also observed in B and C patterns, respectively (30). Slight changes in the spectra were observed in Pattern C, the peaks related to niosome containing zingerone when compared with the control of niosome (without zingerone in Pattern B). As can be seen, in pattern C, peaks at 2919.80, 1736.22, and 2850.44 cm^{-1} when the drug was introduced into the noisome, were slightly changed to 2919.19, 1737. 17, and 2850.10 cm^{-1}, respectively. It can be concluded that between niosome and drug did not occur chemical interaction, and both have kept their nature and stayed away from change. It showed that zingerone had been entrapped in the niosome and had kept its nature.

The MIC and MBC of zingerone and niosome containing zingerone. As demonstrated in (Table 1), the MIC and MBC of niosome containing zingerone were 125 µg ml^{-1} and 250 µg ml^{-1}, respectively while the MIC and MBC of zingerone against MRSA strains were 512 µg ml^{-1} and 1000 µg ml^{-1}, respectively.

Minimum biofilm eradication concentration (MBEC). The free zingerone and zingeron-loaded niosomes eradicated one-day old biofilm at the concentrations of 1000 and 250 µg ml^{-1}, respectively (Table 1). Free zingerone (at × 2 MIC) affected on one-day old biofilm mass, however, niosome contain-

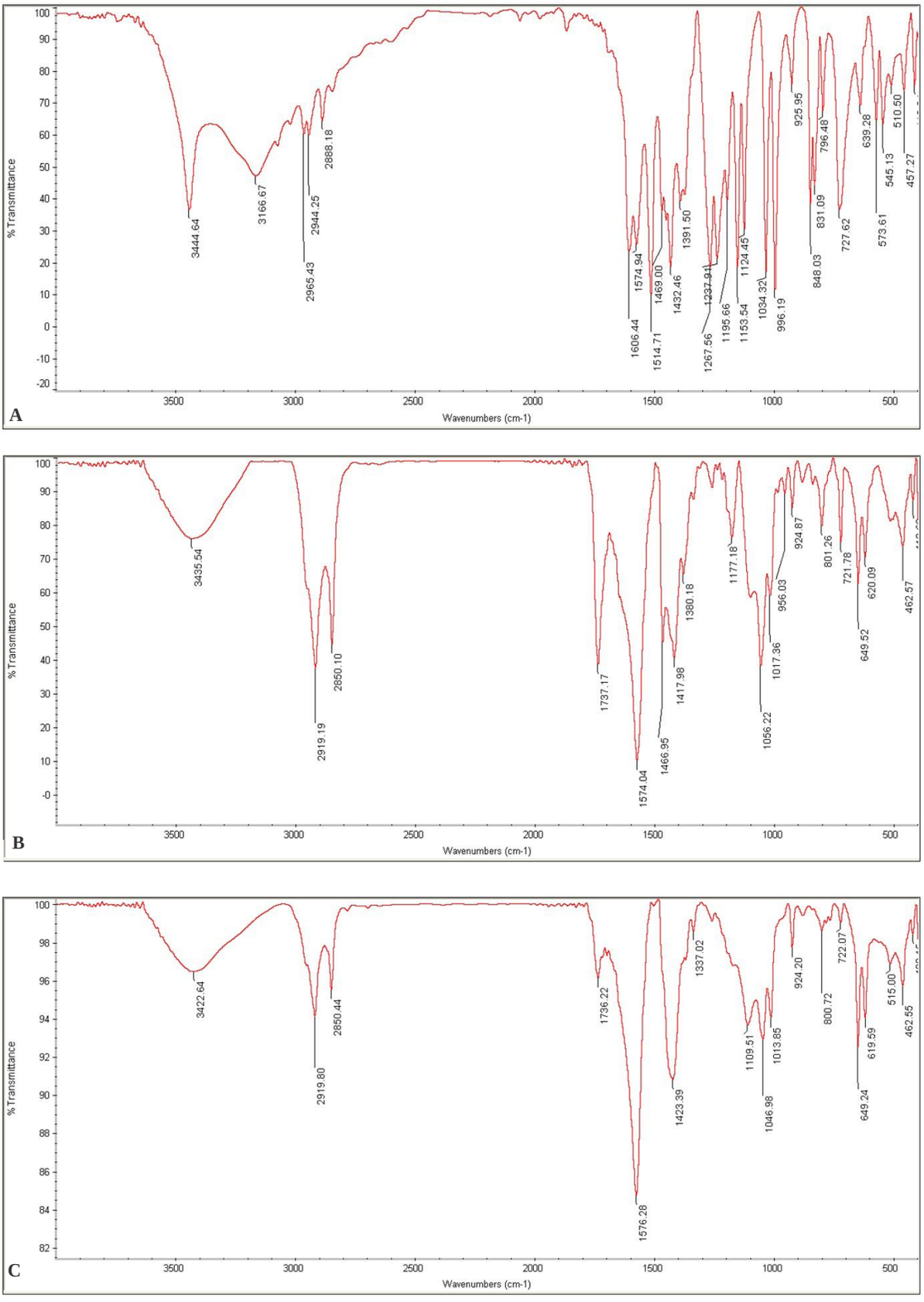

Fig. 3. FTIR spectra (A) free zingerone, (B) niosome without zingerone as control, (C) niosomes containing zingerone.

ing zingerone had substantial effect on-one day old MRSA biofilm (P <0.05). Free zingerone at 1000 µg ml^{-1} eliminated three-days old preestablished biofilm, wherease, niosome containing zingerone affected one three- and five-days old biofilms at concentrations of 250 µg ml^{-1} and 500 µg ml^{-1}, respectively. However, free Zingeron did not significantly affect five-day old biofilm mass. The eradication rate of zingerone and noisome containing zingerone against one, three- and five-days old MRSA biofilms is demonstrated (Fig. 4).

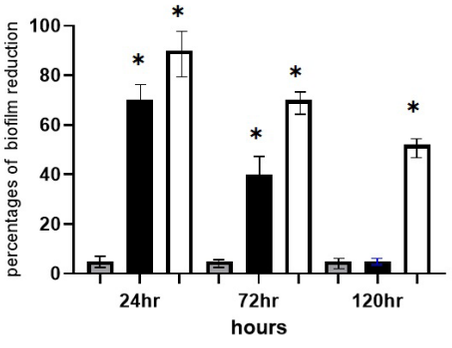

Fig. 4. Eradication rate of zingerone and noisome containing zingerone against one, three- and five-days old MRSA biofilms. Gray bars, control samples treated with TSB medium alone; Black bars, samples treated with Zingerone; White bars, biofilms treated with Zingerone-loaded niosomes. Statistical analysis was done using Student's t-test and the P value < 0.05 was considered as significant (noted with *).

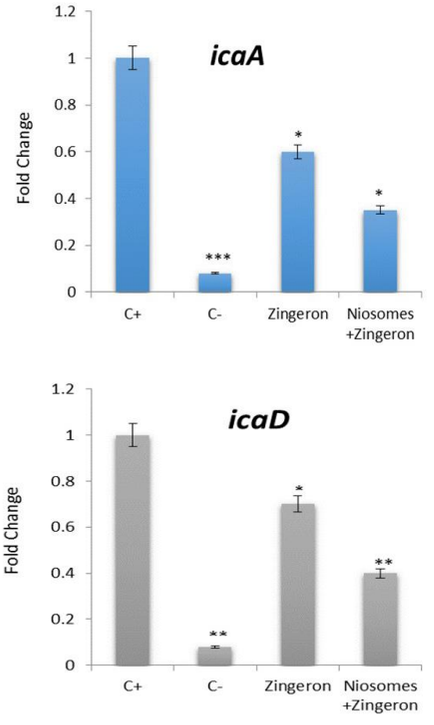

Fig. 5. The effects of Zingerone and Zingerone-loaded niosomes on the expression of the genes responsible for biofilm formation by MRSA. Gene expressions before (C+: positive control) and after treatment have been shown (P < 0.001). Also, C- is a negative control in which biofilm formation was prevented.

According to our results, zingeron-loaded niosomes eradicated 90%, 70% and 55% of one, three- and five-day old MRSA biofilm.

Effect of zingerone and zingerone-loaded niosomes on the expression levels of biofilm-associated genes quantified by real-time PCR. Real-time PCR results indicated that in the presence of zingerone-loaded niosomes, the expression of the biofilm-associated genes (**ica A** and *ica D*) reduced significantly (Fig. 5, P <0.001). However, compared to the positive control, zingerone-loaded niosomes had a 50% reduction in the expressions of *ica A* and *ica D* genes (Fig. 5, P ≤0.01).

DISCUSSION

Methicillin-resistant *Staphylococcus aureus* (MRSA) is a considerable public health problem worldwide, causing significant morbidity and mortality and also raising healthcare expenses (31). MRSA incidence has increased over the last 10 years and is a public health problem in healthcare facilities, sports facilities, clinics, and the community. In recent year, MRSA was known as a high-priority pathogen, causing drastic challenges in healthcare systems (32, 33). The biofilm formation ability of staphylococci has for decades been identified as the most frequent cause of biofilm-associated infections with *S. epidermidis* and *S. aureus* and is closely associated to genetic lineages, multidrug-resistance profiles, and highly virulent strains (31). Our results indicated that MRSA isolates have a high ability for biofilm formation, which has a significant role in decempent of resistant and recurrent infections.

Nanoparticles are considered as a suitable and promising drug delivery system to control the formation of microcolonies and biofilms. Niosomes as lipid nanoparticles are known as drug carriers for various reasons including controlling and slowing

drug release, protecting pharmaceutical molecules, small size, ability to cross bio barriers, increasing drug shelf life and being biodegradable and non-toxic. In this study, niosomes were well-organized with morphologically spherical with a mean particle size of 196 nm. It is indicated that the small size of niosomal particles enhanced antibacterial activity (34, 35). Zingerone with the formula 4-(4- hydroxy-3-methyl phenyl) butane is one of the active compounds of ginger root which is used in the food industry as a flavoring and seasoning and also is a natural, herbal, and non-toxic compound (36). Due to the development of resistant bacteria to almost all existent antibiotics (37), the use of natural compounds such as zingerone can be a promising solution for the treatment of chronic infections caused by MRSA biofilm.

According to the results of the current study, niosome containing zingerone had a spherical morphology with an average diameter of 196.1 nm. It is indicated that the smaller size of nanoparticles leads to more effective antibacterial activity (38). Additionally, the zeta potential of -37.3 mV implied high stability of our noisome containing zingerone because the absolute zeta potential of 30 mV and higher showed more stability and appropriate dispersion due to electrostatic repulsion (39). Despite the small size of our niosome, the percentage of zingerone entrapment in the primary noisome containing zingerone batch was calculated at 69.1%. This high entrapment efficiency can result from its formulation containing span60 and cholesterol. It is proven that the entrapment efficiency is considerably affected by the type and amount of surfactant as well as the surfactant/cholesterol ratio (40). The length of the alkyl chain of used surfactants is a significant factor affecting the permeability of niosomes for zingerone entrapment and consequently on their antimicrobial effectiveness (42).

In the present study, noisomes containing zingerone compared to free zingerone, significantly affected the pre-formed biofilm of MRSA isolates. The amount of zingerone MIC was drastically reduced when encapsulated in niosomes. In 2014, Barakat et al. (41) investigated the effect of niosomes containing vancomycin on the inhibition of *S. aureus* biofilm. They stated that using niosomes as nano carriers is a new approach to inhibit the formation of *S. aureus* biofilm. In 2020, Kashef et al. (43), investigated the antimicrobial and anti-biofilm activity of niosomes containing ciprofloxacin against 59 clinical *S. aureus* isolates. The results revealed that in more than 62% of isolates, MBIC and MBEC niosome form of ciprofloxacin compared to free ciprofloxacin decreased. In 2021, Zafari et al. (18) investigated the anti-biofilm activity of niosomes containing cefazolin against MRSA strains. The *in vitro* results showed that niosomes containing cefazolin were significantly removed one, three- and five-day old MRSA biofilms. The results of the present study confirmed the results of the researches that we mentioned and in addition, provided a new idea and strategy for the treatment of infections associated with MRSA biofilms, especially in the treatment of diabetic wounds. Therefore, using Niosomal Zingerone can be a promising solution for the treatment of chronic infections caused by MRSA biofilm.

CONCLUSION

Zingerone-loaded niosomes offer an alternative approach to the treatment of human biofilm-associated infections. To our knowledge, this is the first report on the eradication of MRSA formed biofilms by Zingerone-loaded niosomes. Further investigations will be necessary to assess the safety and efficacy of the niosomes for a potential application in clinical trials.

REFERENCES

1. Vazquez-Sanchez D, Rodriguez-Lopez P (2018). Biofilm Formation of *Staphylococcus aureus. Staphylococcus aureus* pp. 87-103.
2. Petrelli D, Repetto A, D'Ercole S, Rombini S, Ripa S, Prenna M, et al. Analysis of meticillin-susceptible and meticillin-resistant biofilm-forming *Staphylococcus aureus* from catheter infections isolated in a large Italian hospital. *J Med Microbiol* 2008; 57: 364-372.
3. Shafiei M, Abdi-Ali A, Shahcheraghi F, Vali H, Shahbani Zahiri H, Akbari Noghabi K. Analysis of *Pseudomonas aeruginosa* PAO1 biofilm protein profile after exposure to n-butanolic Cyclamen coum extract alone and in combination with ciprofloxacin. *Appl Biochem Biotechnol* 2017; 182: 1444-1457.
4. Safaei M, Maleki H, Soleimanpour H, Norouzy A, Zahiri HS, Vali H, et al. Development of a novel method for the purification of C-phycocyanin pigment from a local cyanobacterial strain Limnothrix sp. NS01 and evaluation of its anticancer properties. *Sci Rep* 2019; 9: 9474.
5. Namvar AE, Asghari B, Ezzatifar F, Azizi G, Lari AR. Detection of the intercellular adhesion gene cluster

(*ica*) in clinical *Staphylococcus aureus* isolates. *GMS Hyg Infect Control* 2013; 8: Doc03.
6. Gad GF, El-Feky MA, El-Rehewy MS, Hassan MA, Abolella H, El-Baky RM. Detection of *icaA, icaD* genes and biofilm production by *Staphylococcus aureus* and *Staphylococcus epidermidis* isolated from urinary tract catheterized patients. *J Infect Dev Ctries* 2009; 3: 342-351.
7. Vallet I, Olson JW, Lory S, Lazdunski A, Filloux A. The chaperone/usher pathways of *Pseudomonas aeruginosa:* identification of fimbrial gene clusters (cup) and their involvement in biofilm formation. *Proc Natl Acad Sci U S A* 2001; 98: 6911-6916.
8. Choi Y-S, Kim C, Moon J-H, Lee J-Y. Removal and killing of multispecies endodontic biofilms by N-acetylcysteine. *Braz J Microbiol* 2018; 49: 184-188.
9. Tavano L, Gentile L, Oliviero Rossi C, Muzzalupo R. Novel gel-niosomes formulations as multicomponent systems for transdermal drug delivery. *Colloids Surf B Biointerfaces* 2013; 110: 281-288.
10. Aparajay P, Dev A. Functionalized niosomes as a smart delivery device in cancer and fungal infection. *Eur J Pharm Sci* 2022; 168: 106052.
11. Ahmad B, Rehman MU, Amin I, Ahmad SB, Farooq A, Muzamil S, et al. Zingerone (4-(4-hydroxy-3-methylphenyl) butan-2-one) protects against alloxan-induced diabetes via alleviation of oxidative stress and inflammation: probable role of NF-kB activation. *Saudi Pharm J* 2018; 26: 1137-1145.
12. Shamsabadi S, Nazer Y, Ghasemi J, Mahzoon E, Rahimi VB, Ajiboye BO, et al. Promising influences of zingerone against natural and chemical toxins: A comprehensive and mechanistic review. *Toxicon* 2023; 233: 107247.
13. Seth AK, Geringer MR, Nguyen KT, Agnew SP, Dumanian Z, Galiano RD, et al. Bacteriophage therapy for *Staphylococcus aureus* biofilm–infected wounds: a new approach to chronic wound care. *Plast Reconstr Surg* 2013; 131: 225-234.
14. Humphries R, Bobenchik AM, Hindler JA, Schuetz AN. Overview of changes to the clinical and laboratory standards institute performance standards for antimicrobial susceptibility testing, M100, 31st Edition. *J Clin Microbiol* 2021; 59(12): e0021321.
15. Shafiei M, Abdi Ali A, Shahcheraghi F, Saboora A, Akbari Noghabi K. Eradication of *Pseudomonas aeruginosa* biofilms using the combination of n-butanolic cyclamen coum extract and ciprofloxacin. *Jundishapur J Microbiol* 2014; 7(2): e14358.
16. Kim M-H, Yamayoshi I, Mathew S, Lin H, Nayfach J, Simon SI. Magnetic nanoparticle targeted hyperthermia of cutaneous *Staphylococcus aureus* infection. *Ann Biomed Eng* 2013; 41: 598-609.
17. Antunes BP, Moreira AF, Gaspar VM, Correia IJ. Chitosan/arginine–chitosan polymer blends for assembly of nanofibrous membranes for wound regeneration. *Carbohydr Polym* 2015; 130: 104-112.
18. Zafari M, Adibi M, Chiani M, Bolourchi N, Barzi SM, Shams Nosrati MS, et al. Effects of cefazolin-containing niosome nanoparticles against methicillin-resistant *Staphylococcus aureus* biofilm formed on chronic wounds. *Biomed Mater* 2021; 16: 035001.
19. Shamkani F, Barzi SM, Badmasti F, Chiani M, Mirabzadeh E, Zafari M, et al. Enhanced anti-biofilm activity of the minocycline-and-gallium-nitrate using niosome wrapping against *Acinetobacter baumannii* in C57/BL6 mouse pneumonia model. *Int Immunopharmacol* 2023; 115: 109551.
20. Jacob S, Nair AB, Al-Dhubiab BE. Preparation and evaluation of niosome gel containing acyclovir for enhanced dermal deposition. *J Liposome Res* 2017; 27: 283-292.
21. Sabaeifard P, Abdi-Ali A, Soudi MR, Dinarvand R. Optimization of tetrazolium salt assay for *Pseudomonas aeruginosa* biofilm using microtiter plate method. *J Microbiol Methods* 2014; 105: 134-140.
22. Petit T, Puskar L. FTIR spectroscopy of nanodiamonds: Methods and interpretation. *Diam Relat Mater* 2018; 89: 52-66.
23. Faghihzadeh F, Anaya NM, Schifman LA, Oyanedel-Craver V. Fourier transform infrared spectroscopy to assess molecular-level changes in microorganisms exposed to nanoparticles. *Nanotechnol Environ Eng* 2016; 1: 1-16.
24. Wiegand I, Hilpert K, Hancock RE. Agar and broth dilution methods to determine the minimal inhibitory concentration (MIC) of antimicrobial substances. *Nat Protoc* 2008; 3: 163-175.
25. Robertson J, McGoverin C, White JR, Vanholsbeeck F, Swift S. Rapid detection of *Escherichia coli* antibiotic susceptibility using live/dead spectrometry for lytic agents. *Microorganisms* 2021; 9: 924.
26. Thammawithan S, Siritongsuk P, Nasompag S, Daduang S, Klaynongsruang S, Prapasarakul N, et al. A biological study of anisotropic silver nanoparticles and their antimicrobial application for topical use. *Vet Sci* 2021; 8: 177.
27. Gopalakrishnan S, Gupta A, Makabenta JMV, Park J, Amante JJ, Chattopadhyay AN, et al. Ultrasound-enhanced antibacterial activity of polymeric nanoparticles for eradicating bacterial biofilms. *Adv Healthc Mater* 2022; 11(21): e2201060.
28. Allkja J, van Charante F, Aizawa J, Reigada I, Guarch-Perez C, Vazquez-Rodriguez JA, et al. Interlaboratory study for the evaluation of three microtiter plate-based biofilm quantification methods. *Sci Rep* 2021; 11: 13779.
29. Atshan SS, Shamsudin MN, Karunanidhi A, Van Bel-

kum A, Lung LT, Sekawi Z, et al. Quantitative PCR analysis of genes expressed during biofilm development of methicillin resistant *Staphylococcus aureus* (MRSA). *Infect Genet Evol* 2013; 18: 106-112.

30. Afreen U, Fahelelbom KM, Shah SNH, Ashames A, Almas U, Khan SA, et al. Formulation and evaluation of niosomes-based chlorpheniramine gel for the treatment of mild to moderate skin allergy. *J Exp Nanosci* 2022; 17: 467-495.
31. Hosseini M, Shapouri Moghaddam A, Derakhshan S, Hashemipour SMA, Hadadi-Fishani M, Pirouzi A, et al. Correlation between biofilm formation and antibiotic resistance in MRSA and MSSA isolated from clinical samples in Iran: a systematic review and meta-analysis. *Microb Drug Resist* 2020; 26: 1071-1080.
32. Cheung GYC, Bae JS, Otto M. Pathogenicity and virulence of *Staphylococcus aureus. Virulence* 2021; 12: 547-569.
33. Tocco I, Zavan B, Bassetto F, Vindigni V. Nanotechnology-based therapies for skin wound regeneration. *J Nanomater* 2012; 2012: 11.
34. Hedayati Ch M, Abolhassani Targhi A, Shamsi F, Heidari F, Salehi Moghadam Z, Mirzaie A, et al. Niosome-encapsulated tobramycin reduced antibiotic resistance and enhanced antibacterial activity against multidrug-resistant clinical strains of *Pseudomonas aeruginosa*. *J Biomed Mater Res A* 2021; 109: 966-980.
35. Shah P, Goodyear B, Dholaria N, Puri V, Michniak-Kohn B. Nanostructured non-ionic surfactant carrier-based gel for topical delivery of desoximetasone. *Int J Mol Sci* 2021; 22: 1535.
36. Ahmad B, Rehman MU, Amin I, Arif A, Rasool S, Bhat SA, et al. A review on pharmacological properties of zingerone (4-(4-Hydroxy-3-methoxyphenyl)-2-butanone). *ScientificWorldJournal* 2015; 2015: 816364.
37. Madsen JS, Burmølle M, Hansen LH, Sørensen SJ. The interconnection between biofilm formation and horizontal gene transfer. *FEMS Immunol Med Microbiol* 2012; 65: 183-195.
38. Abdelaziz AA, Elbanna TE, Sonbol FI, Gamaleldin NM, El Maghraby GM. Optimization of niosomes for enhanced antibacterial activity and reduced bacterial resistance: *in vitro* and *in vivo* evaluation. *Expert Opin Drug Deliv* 2015; 12: 163-180.
39. Junyaprasert VB, Teeranachaideekul V, Supaperm T. Effect of charged and non-ionic membrane additives on physicochemical properties and stability of niosomes. *AAPS PharmSciTech* 2008; 9: 851-859.
40. Khan DH, Bashir S, Figueiredo P, Santos HA, Khan MI, Peltonen L. Process optimization of ecological probe sonication technique for production of rifampicin loaded niosomes. *J Drug Deliv Technol* 2019; 50: 27-33.
41. Barakat HS, Kassem MA, El-Khordagui LK, Khalafallah NM. Vancomycin-eluting niosomes: a new approach to the inhibition of staphylococcal biofilm on abiotic surfaces. *AAPS PharmSciTech* 2014; 15: 1263-1274.
42. Rahimipour S, Salahinejad E, Sharifi E, Nosrati H, Tayebi L. Structure, wettability, corrosion and biocompatibility of nitinol treated by alkaline hydrothermal and hydrophobic functionalization for cardiovascular applications. *Appl Surf Sci* 2020; 506: 144657.
43. Kashef MT, Saleh NM, Assar NH, Ramadan MA. The antimicrobial activity of ciprofloxacin-loaded niosomes against ciprofloxacin-resistant and biofilm-forming *Staphylococcus aureus. Infect Drug Res* 2020; 13: 1619-1629.